Experimental Tests of Thin RC U-shaped Walls with a Single Layer of Reinforcement

Ryan D. Hoult[1], Aaron Appelle[2], João P. Almeida[3] and Katrin Beyer[4]

1. Corresponding Author. Postdoctoral Researcher, Department of Infrastructure Engineering, The University of Melbourne, Parkville, VIC 3010, Australia. Email: ryan.hoult@unimelb.edu.au

2. Master Student, Earthquake Engineering and Structural Dynamics Laboratory, École Polytechnique Fédérale de Lausanne, Switzerland. Email: appellea@stanford.edu

3. Professor, Institute of Mechanics, Materials and Civil Engineering, Université catholique de Louvain, Belgium. Email: joao.almeida@uclouvain.be

4. Professor, Earthquake Engineering and Structural Dynamics Laboratory, École Polytechnique Fédérale de Lausanne, Switzerland. Email: katrin.beyer@epfl.ch

Abstract

Reinforced concrete (RC) U-shaped core walls are commonly used in buildings to provide lateral resistance for wind and earthquake actions. While there is an abundance of these structural elements within the building stocks of both low-to-moderate and high seismic regions, there have been few experimental studies focusing on the seismic resistance of RC walls with a U-shaped cross-section. Building codes in some Latin American countries, such as Colombia, currently allow very thin RC walls with a single layer of reinforcement to be constructed. This type of construction is similar to practices in Australia, prior to the revised Concrete Structures building code coming into effect in 2019. Large-scale tests of two thin RC U-shaped walls with a single layer of vertical reinforcement were conducted in the Earthquake Engineering Structural Dynamics Laboratory at École Polytechnique Fédérale de Lausanne (EPFL), Switzerland. This paper presents some of the test setups and loading protocols used to test the walls, as well as the initial results, including local and global failure modes.

Keywords: shear, U-shaped, C -shaped, out-of-plane, buckling, slender

INTRODUCTION

Reinforced concrete (RC) shear (or structural) walls are commonly used in RC buildings to provide the lateral stability from wind and earthquakes. A popular choice in construction is to use U-shaped, or C-shaped, walls for a buildings core, as it can enclose elevators and stairs. Furthermore, the behaviour of non-rectangular RC walls (i.e., U-shaped) differs considerably in comparison to rectangular walls, where the flanged sections increase the lateral strength and stiffness of the wall (Paulay & Priestley, 1992). There is currently a proliferation of mid- and high-rise RC buildings in some Latin American countries, including Colombia. Some concerns have been raised by engineers internationally as to the effectiveness of the RC walls that are being designed and built in Colombia, as the building code currently allows the use of slender (or thin) walls with a single layer of longitudinal reinforcement. For example, it is anticipated that most of the RC walls that have recently been embedded in buildings throughout Colombia have thicknesses ranging from as low as 70 mm (Blandón *et al.*, 2018) and up to 150 mm (Rosso *et al.*, 2018). These walls are commonly unconfined with a single-layer of vertical reinforcement (Rosso *et al.*, 2018) and are also designed for low concrete strengths (f'_c) typically ranging from 21 MPa to 35 MPa (Mejia *et al.*, 2004). Furthermore, a minimum longitudinal reinforcement ratio (ρ_{wv}) of just 0.25% is required by the building codes in Colombia for RC walls (Arteta *et al.*, 2017); this is low considering the amount typically required to cause secondary cracking and ensure a ductile response of the wall is achieved in the event of an earthquake (Hoult *et al.*, 2018a; Hoult *et al.*, 2018b). This type of construction is not dissimilar to recent construction practices in Australia, where there have been some concerns with regard to the performance of precast walls with single layers of reinforcement (Goldsworthy *et al.*, 2015). With the recent revision of AS 3600:2018 (Standards Australia, 2018), it is expected that the design and construction of 'limited-ductile' walls, corresponding to a ductility (μ) of 2, will *at least* have two layers of longitudinal reinforcement and with a minimum thickness of 200 mm.

Given that Colombia includes regions of high seismicity, RC buildings therein are at risk to experiencing a moderate-to-large earthquake event within the lifetime of the structure. It is feared that buildings that utilise thin and unconfined RC walls with a single layer of longitudinal reinforcement will perform poorly in the event of a moderate to large earthquake event. However, there is a paucity of experimental testing that has been conducted on RC U-shaped walls. While the authors concede that has been some recent efforts to conduct experimental testing on these elements (Behrouzi *et al.*, 2018; Beyer *et al.*, 2008; Constantin & Beyer, 2016), there is virtually no evidence for the seismic performance of unconfined RC U-shaped walls with a single layer of reinforcement.

To investigate the seismic performance of such elements, an experimental program was conducted at the *Earthquake Engineering and Structural Dynamics Laboratory (EESD Lab)*, *École Polytechnique Féderale de Lausanne (EPFL)*, Switzerland testing two full scale RC U-shaped wall specimens. One of the primary objectives of these tests is to observe if out-of-plane instability is an issue for RC U-shaped walls designed to similar construction practices in Colombia and other Latin American countries. Out-of-plane failures of ductile RC walls have been observed in recent earthquake events (Maffei *et al.*, 2014; Sritharan *et al.*, 2014). It is believed that the current design practice in

Colombia, coupled with the seismic behaviour of U-shaped walls, could have the potential to result in out-of-plane instability.

This paper presents the design of two U-shaped wall specimens tested. Some of the initial experimental observations and results of one of the specimens are discussed, which includes estimates of the plastic hinge lengths of the wall. For the sake of brevity, the testing and results of specimen TUE will be primarily discussed in this paper, whereas the interested reader is encouraged to look for the corresponding journal publication expected early in 2020.

1. Specimen TUE and TUF

The reinforcement layout and cross-section of the two specimens tested in the EESD laboratory at EPFL, denoted as specimens TUE (Test Unit E) and TUF (Test Unit F), are given in Figure 1a. Both wall specimens had the same geometry and reinforcement detailing, which included lumped longitudinal reinforcing bars of 16 mm diameter in the boundary ends of the flange and intersecting web-flange regions. The vertical reinforcement in between boundary regions consisted of 6 mm diameter bars spaced at 100 mm, which was also used for the horizontal (shear) reinforcement. The shear span of the walls, illustrated in Figure 1b, was 4250 mm in the north-south (NS) direction, while in the east-west direction the shear span was 4650 mm. This resulted in shear span ratios ($M/VL_w = H_e/L_w$) of 4.05 and 3.58 for the NS and EW directions, respectively.

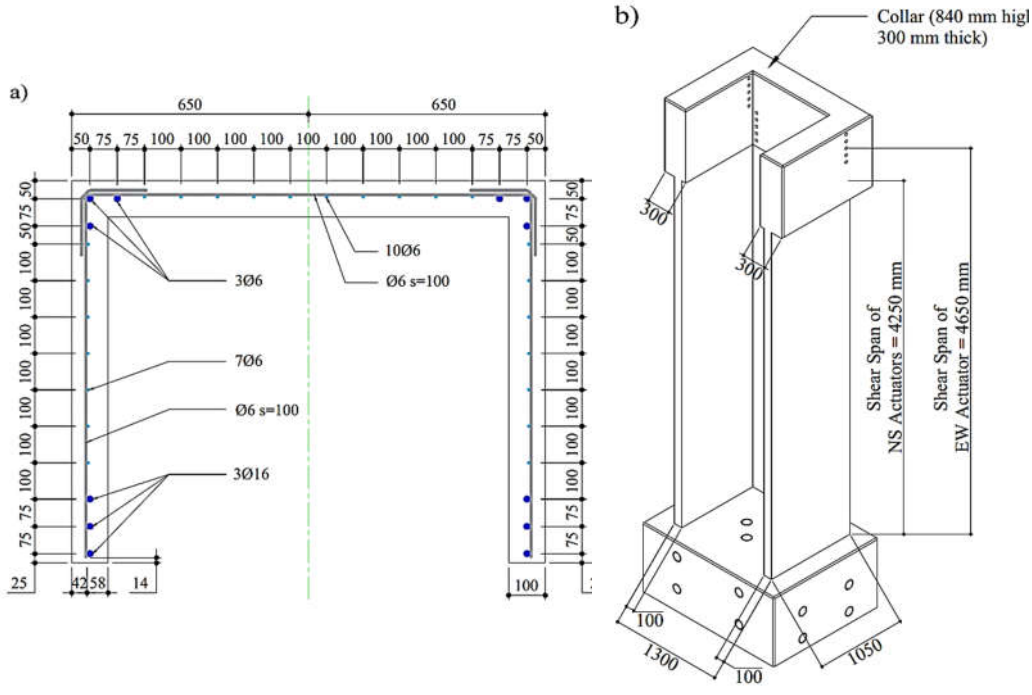

Figure 1 Test units TUE and TUF: (a) cross-section and reinforcement layout and (b) elevation view (not to scale)

The instrumentation used during testing is illustrated in Figure 2b. It included Linear Variable Differential Transformers (LVDTs) to measure displacement at the top of the wall, light emitting diodes (LEDs) to track the wall profile on the boundary ends of the

flanges, and a system of Digital Image Correlation (DIC) to record displacements and strains on the exterior wall faces.

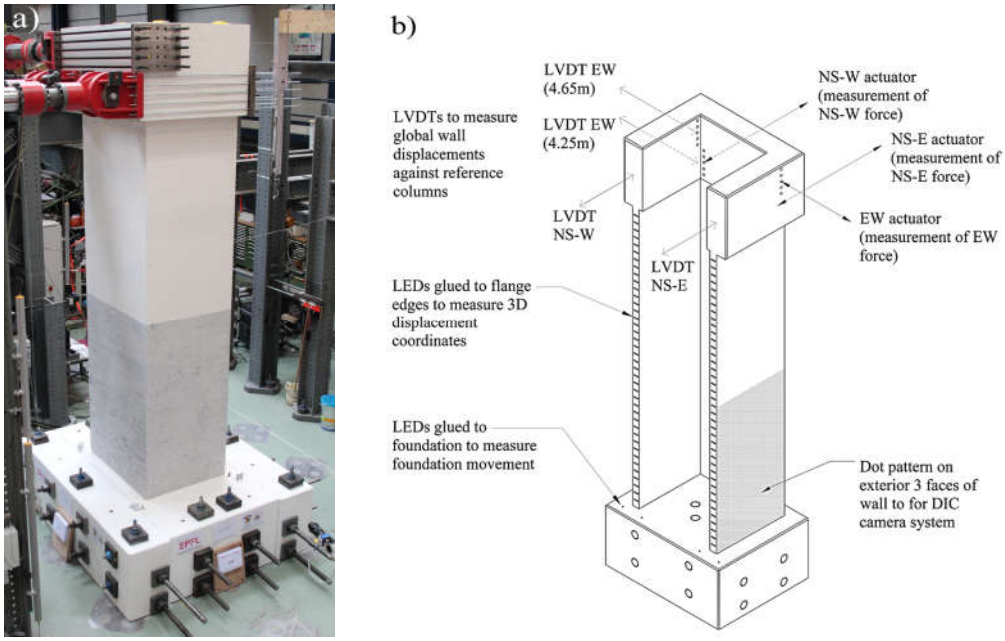

Figure 2 (a) Test setup of TUE and (b) location of conventional and optical measurement devices (dimensions in mm)

As stated in the introduction, one of the primary objectives of this experimental study is to observe if out-of-plane instability is an issue for slender RC U-shaped walls that have a single-layer of vertical reinforcement. Hence, the reverse-cyclic loading protocol for TUE and TUF were chosen to prevent a premature crushing-type failure due to compression; this type of failure in non-rectangular RC walls is well documented from previous experiments (Constantin & Beyer, 2014). As such, the loading directions that caused the wall to have a large compression zone were limited for this study. For example, the drift level was limited for the wall bending about its minor axis when the web is in tension, thus avoiding a large compression depth and correspondingly large compression strains at the boundary ends.

For specimen TUE, in-plane loading was applied to the wall, which corresponds to Positions A, B, C and D in Figure 3b. The loading history for TUE is described below and shown in Figure 4:

- 0.0% - 0.4% drift: O-D-C-O-B-A-O, one cycle (increments of 0.1% drift)
- 0.5% - 1.2% drift: O-D-C*-O-B-A-O, two cycles (increments of 0.1% drift)
- 1.2% - 2.0% drift: O-D-C*-O-B-A-O, two cycles (increments of 0.2% drift)
- 2.0% - 3.0% drift: O-D-C*-O-B-A-O, two cycles (increments of 0.5% drift)

* Position C is limited to 0.4% drift

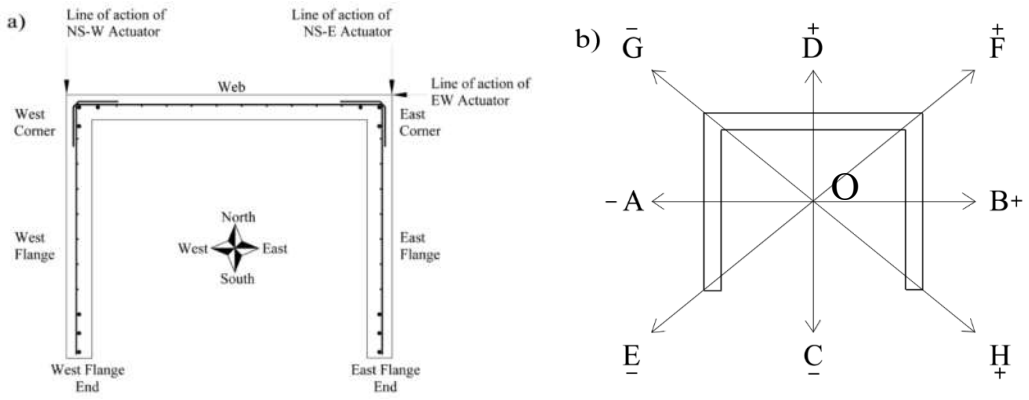

Figure 3 (a) cardinal points, sign convention for forces and displacements, wall parts and (b) loading positions

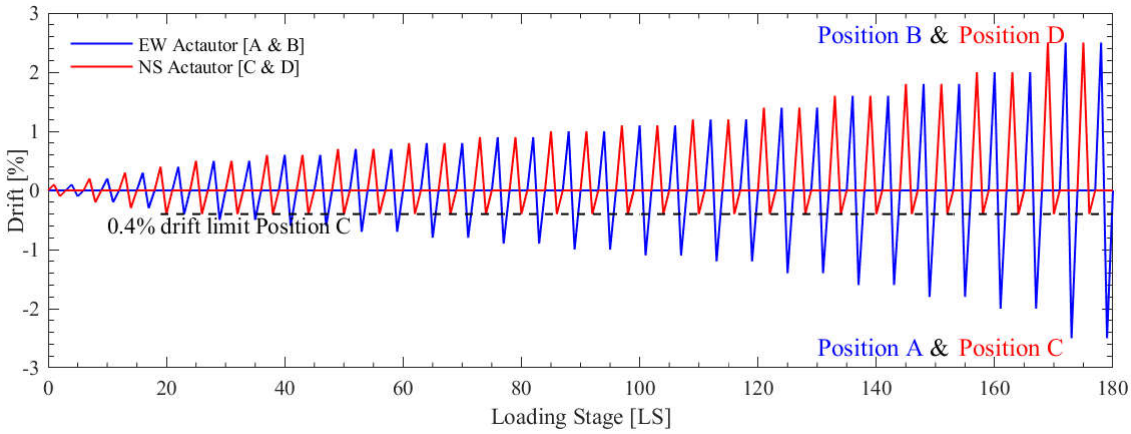

Figure 4 Loading history for specimen TUE

2. Experimental Observations

Some of the experimental observations and findings for specimen TUE are discussed here. The force-displacement relationship is given in Section 3.1. The local and global failure modes of the wall specimen is discussed and shown in Section 3.2. Finally, some estimates of the plastic hinge lengths are given in Section 3.3.

3.1. Force-Displacement Hysteresis

The force-displacement hysteresis for specimen TUE is given in Figure 5. As in-plane loading was used in TUE, the EW actuator (i.e., loading parallel to the web, Figure 3a) force is plotted against the top wall displacement, which was measured by means of the horizontal LVDT recording of EW displacement at h_{EW} = 4.65 m (corresponding to the effective height of the applied actuator in this direction); for the north-south direction (i.e., loading parallel to the flanges), the total force from the NS actuators (NS_E and NS_W, Figure 3a) and the mean top wall displacement are plotted, which have been measured from the LVDTs recording the NS displacements at h_{NS} = 4.25 m.

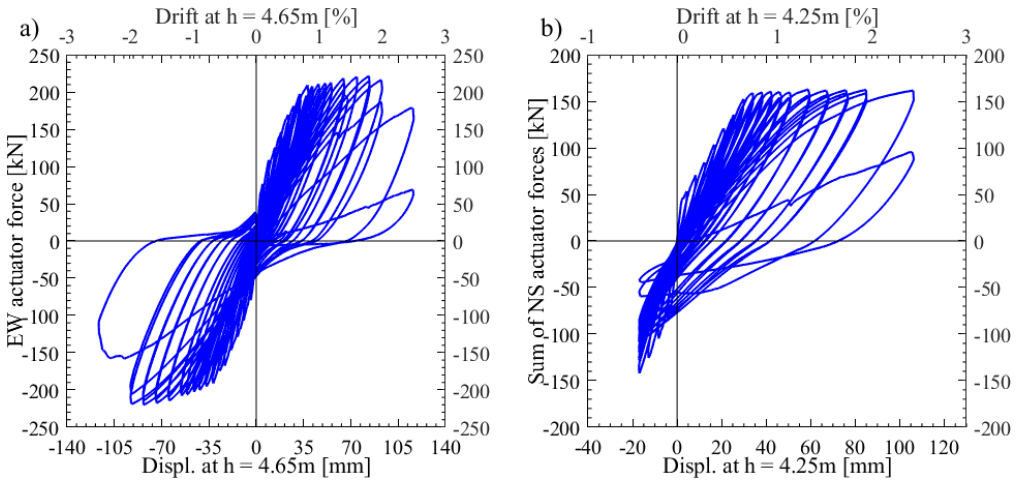

Figure 5 TUE: force-displacement hystereses for (a) east-west direction (Position A and B) and (b) north-south direction (Position C and D)

3.2. Failure modes

The onset of failure of specimen TUE occurred to due to a local out-of-plane buckling in the East flange. This failure occurred during loading in the A-B direction when the East flange was in compression at Position B (Figure 6a). The out-of-plane buckling occurred during the starting stage of the second cycle to reach a drift of 2.0%. Prior to this failure, the wall had reached 2.0% drift in the D-C direction; at Position D, a small compression depth existed over the length of the web, which results in a large tension zone in the flanges, resulting in large tensile inelastic strains in the reinforcement at the boundary ends. A good distribution of cracking up the wall height of the East and West flange, particularly when pushing towards position D, was observed throughout testing. This is primarily due to the lumped reinforcement in the boundary ends and the small thickness of the walls resulting in a high reinforcement ratio and allowing secondary cracking to occur (Hoult *et al.*, 2018a; Hoult *et al.*, 2018b). As the drifts were limited at Position C to avoid a premature compression failure due to the unconfined boundary ends, the lumped reinforcing bars were only subjected to large compression forces once the wall was pushed to Position B, resulting in local out-of-plane buckling at this position.

As no significant reduction in strength had been observed with the out-of-plane buckling in the East flange, the test continued, and a similar out-of-plane buckling of the boundary end of the West flange was observed during loading in the D-C direction for the first cycle of 2.5% drift (Figure 6b). Prior to the West flange failing in this fashion, the wall was pushed to Position D at 2.5% drift, where the lumped longitudinal bars in the boundary of the West flange were subjected to large tensile strains at the distributed and large cracks in the plastic region of the wall, resulting in the out-of-plane buckling observed when returning to Position O and pushing the wall to the limiting drift at Position C.

A large compression strut in the web leading down to this region (the “toe” of the wall) was observed throughout the test, where a large crack in the web (≈5-7 mm) was present once the boundary end of the East flange had buckled. As testing continued after observing the localised out-of-plane buckling failures, the concrete crushed in the corners of the web-flange regions during the second cycles of 2.5% drift to Positions A, B and D, resulting in shear-sliding along a primary crack in the web and ultimately

the loss of concrete within the web (Figure 6c). The crushing of concrete, shear sliding and complete loss of concrete in the web resulted in a drastic drop in shear strength (≈72%), where the testing of TUE was stopped.

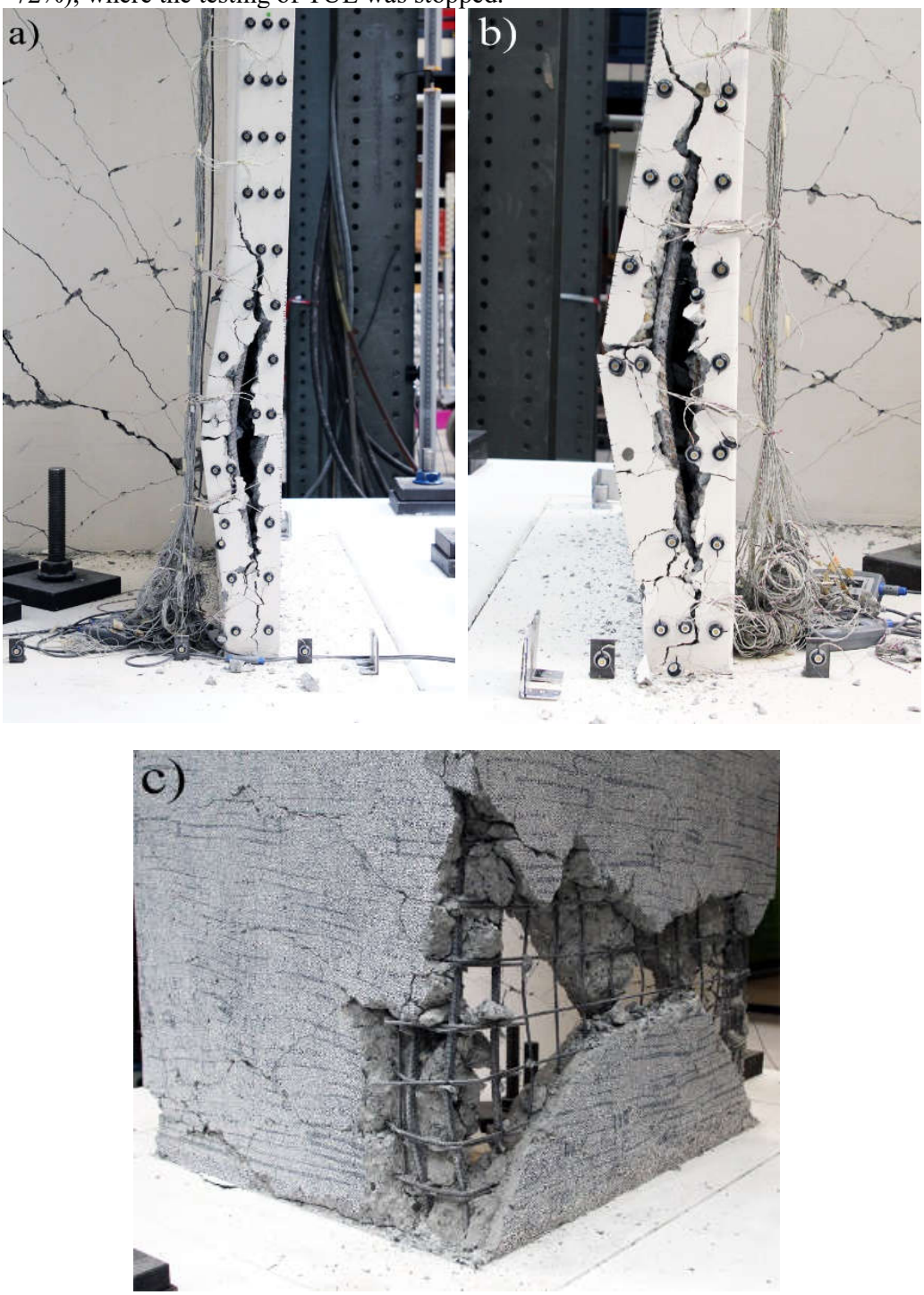

Figure 6 Out-of-plane buckling observed in (a) East flange during loading to Position B at 2.0% drift (b) West flange during loading to Position C after reaching 2.5% drift at Position D and(c) condition of the web at the end of testing

3.3. Plastic Hinge Lengths

Using the displacement data for each of the LEDs at the end of the East Flange, it is possible to estimate the plastic hinge length (L_p) for wall specimen TUE when it is pushed to Position D (i.e., Figure 3b, when the flange ends are the extreme tension fibre regions and the web of the wall is under compression). Although the plastic strains in the boundary regions of the flange will vary up the wall height at this position, it is common practice to simply assume that the inelastic plasticity (and curvature) is uniform for a height above the base that is equivalent to L_p. The plastic hinge length is an important parameter for determining the displacement capacity of RC walls when using the plastic hinge analysis method (Hoult *et al.*, 2018c).

Using the vertical strains of the boundary ends of the East Flange, obtained from one of the three columns of LEDs, the curvature (Φ) distribution up the height of the wall was calculated for different drift levels and assuming a compression depth (c) of half the wall thickness (i.e., 50 mm) (Equation 1). The small compression depth assumed here is reasonable because at Position D the compression from flexural actions will be resisted by the large web area, due to the large web length, and thus a small compression zone should exist.

$$\Phi = \varepsilon_t/(L_f - c) \quad (1)$$

where L_f is the length of the flange and ε_t is the tension strain found from the LEDs at the boundary end of the East flange.
If a linear curvature profile is assumed, then the yield curvature (Φ_y) can be estimated using Equation 2 from Hoult *et al.* (2018c) and Sullivan *et al.* (2012), which is specifically for RC U-shaped walls bending about the minor axis with web in compression (i.e., Position D).

$$\Phi_y = 1.4\varepsilon_{sy}/L_f \quad (2)$$

where ε_{sy} is the yield strain of the steel (≈0.0027).

The curvature distribution up the height of the boundary end of the East flange is given in Figure 7a for different drift levels.

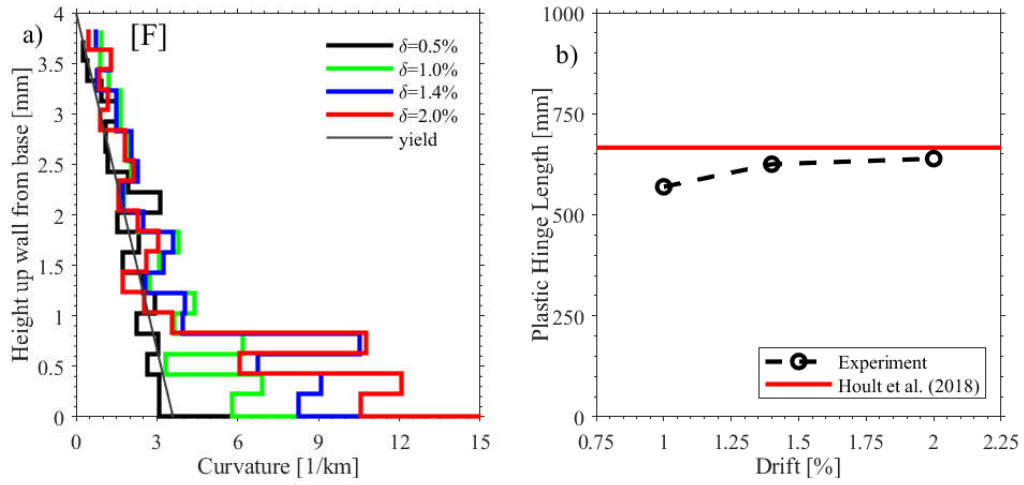

Figure 7 (a) curvature distribution up the height of the boundary end of the East flange of TUE and (b) plastic hinge length estimates for TUE at Position D

The plastic hinge length can be calculated using the Equivalent Plastic Hinge Length (EPHL) method, which has been used in various studies (Hoult *et al.*, 2018a; Hoult *et al.*, 2018b; Kazaz, 2013). The EPHL method uses Equation 3 to transform the area of plastic curvatures, subtracting the area from the assumed linear yield curvature profile, up the wall height and transforming it to an equivalent rectangular area over height L_p.

$$L_p = \frac{1}{\Phi_u - \Phi_y} \int_0^H \left| \Phi(z) - \Phi_y(z) \right| \quad 3$$

where Φ_u is the ultimate curvature found up the wall height for each drift level, $\Phi(z)$ is the curvature up the wall height z, $\Phi_y(z)$ is the yield curvature up the wall height z and H is the full height of the wall.

Using the experimental curvature results and Equation 3, the L_p was calculated for three drifts levels and illustrated in Figure 7b. It should be noted that the L_p was not calculated for a drift of 0.5% as it was shown in Figure 7a to be approximated to the yield curvature profile, and thus it is estimated that no plastic hinge had formed at this level of drift. The L_p values in Figure 7b are shown to slightly increase with level of drift, with a maximum value of 639 mm at a drift of 2.0%, prior to out-of-plane buckling occurring in the East flange. For comparison, the L_p expression in Hoult *et al.* (2018b) is used here (Equation 4), as the expression was specifically derived for unconfined RC U-shaped walls bending about the minor axis with web in compression (i.e., at Position D). The comparison with the equation from Hoult *et al.* (2018b) in Figure 7b shows that the expression provides a very good estimate with that derived experimentally (666 mm).

$$L_p = (0.5L_f - 0.015H_e)(1 - 3\text{ALR})(1.6e^{-0.1\nu}) \leq L_f \quad 4$$

Where L_f is the length of the flange, H_e is the effective height of the wall, ALR is the axial load ratio and υ is the shear stress parameter equivalent to $\tau/0.17\sqrt{f_c'}$. It should be noted that τ is the average shear stress parameter, which can be calculated from a sectional analysis (moment-curvature analysis) or can be estimated by using a simplified approach, which involves dividing the base shear (V_b) of the wall by the gross cross-sectional area of the wall (A_g) (Krolicki *et al.*, 2011).

3. Conclusions

Wall specimen TUE was tested at EPFL in the EESD laboratory for in-plane loading in an attempt to observe if out-of-plane instability could be a problem for RC U-shaped walls with a single layer of reinforcement. The failure mechanisms indicate that once the lumped boundary reinforcement is subjected to a sufficient amount of yielding and plasticity, it has the potential to buckle and cause a localised out-of-plane failure of the flanges. In this case, the initiation of the wall failing was caused by these local failures, where the lumped vertical reinforcement buckled at the ends of the flange before crushing of the wall could occur; however, the potential for a crushing-type failure was significantly reduced by subjecting the wall to no axial load and limited drift cycles in the in-plane direction that causes the largest compression zone. Thus, these types of structural, lateral-load-resisting elements can be prone to some out-of-plane instability. These initial results emphasise the importance of (i) two layers of longitudinal reinforcement in the wall and (ii) confinement in the boundary ends, which will not only reduce bar buckling and the potential for out-of-plane instability, but also increase the compression capacity of the wall in these critical regions. However, it is virtually

impossible to achieve these design considerations (i.e., two layers of reinforcement and confinement) in Colombia and other South American countries if the corresponding design codes continue to allow 70 – 150 mm thick walls to be designed.

The plastic hinge length expression from Hoult *et al.* (2018b) indicates that it provides a good estimate of the equivalent plastic hinge length derived from the experimental LED results. As only some of the LED data has been processed as of writing this paper, it will be interesting to use the data from the digital image correlation (DIC) techniques to (i) further verify the plastic hinge length in this direction and (ii) derive the equivalent plastic hinge length for the other directions of applied load. The authors look forward to publishing these results, along with the results of the second U-shaped wall specimen (TUF), in early 2020.

4. Acknowledgements

The authors would like to acknowledge the support of the Swiss Government Excellence Postdoctoral Scholarship for the year 2018/2019, the Fullbright Program and the funding provided through the Swiss Bilateral Research Programs for the Latin American Region through the one-year research merger scheme. The authors would also like to thank our partners from Colombia, including Carlos Blandón Uribe from Universidad EIA, Carlos Arteta and Gustavo Rodriguez from Universidad del Norte, Ricardo Bonett from Universidad de Medellín, Ana B. Acevedo Jaramillo from Universidad EAFIT, Mario E. Rodriguez from Universidad Nacional Autónoma de México.

5. References

Arteta, C., Sánchez, J., Daza, R., Blandón, C., Bonett, R., Carrillo, J., & Vélez, J. (2017). *Global and local demand limits of thin reinforced concrete structural wall building systems.* Paper presented at the 16th world conference on earthquake engineering. Santiago, Chile.

Behrouzi, A., Mock, A., Lehman, D., Lowes, L., & Kuchma, D. (2018, June 25-29, 2018). *Seismic Performance of Slender C-shaped Walls Subjected to Uni- and Bi-directional Loading.* Paper presented at the Eleventh U.S. National Conference on Earthquake Engineering, Losa Angeles, California.

Beyer, K., Dazio, A., & Priestley, M. J. N. (2008). Quasi-Static Cyclic Tests of Two U-Shaped Reinforced Concrete Walls. *Journal of Earthquake Engineering, 12*(7), 1023-1053. doi:10.1080/13632460802003272

Blandón, C. A., Arteta, C. A., Bonett, R. L., Carrillo, J., Beyer, K., & Almeida, J. P. (2018). Response of thin lightly-reinforced concrete walls under cyclic loading. *Engineering Structures, 176*, 175-187. doi:https://doi.org/10.1016/j.engstruct.2018.08.089

Constantin, R., & Beyer, K. (2014). *Non-rectangular RC walls: A review of experimental investigations*. Paper presented at the 2nd European Conference on Earthquake Engineering and Seismology, Istanbul, Turkey.

Constantin, R., & Beyer, K. (2016). Behaviour of U-shaped RC walls under quasi-static cyclic diagonal loading. *Engineering Structures, 106*, 36-52. doi:http://dx.doi.org/10.1016/j.engstruct.2015.10.018

Goldsworthy, H. M., McBean, P., & Somerville, P. (2015). *Mitigation of Seismic Hazard in Australia by Improving the Robustness of Buildings.* Paper presented at the 10th Pacific Conference on Earthquake Engineering, Sydney, Australia.

Hoult, R., Goldsworthy, H., & Lumantarna, E. (2018a). Plastic Hinge Length for Lightly Reinforced Rectangular Concrete Walls. *Journal of Earthquake Engineering, 22*(8), 1447-1478. doi:10.1080/13632469.2017.1286619

Hoult, R., Goldsworthy, H. M., & Lumantarna, E. (2018b). Plastic Hinge Length for Lightly Reinforced C-shaped Concrete Walls. *Journal of Earthquake Engineering*, 1-32. doi:10.1080/13632469.2018.1453419

Hoult, R. D., Goldsworthy, H. M., & Lumantarna, E. (2018c). Plastic hinge analysis for lightly reinforced and unconfined concrete structural walls. *Bulletin of Earthquake Engineering, 16*(10), 4825-4860. doi:10.1007/s10518-018-0369-x

Kazaz, l. (2013). Analytical Study on Plastic Hinge Length of Structural Walls. *Journal of Structural Engineering*(11), 1938.

Krolicki, J., Maffei, J., & Calvi, G. M. (2011). Shear Strength of Reinforced Concrete Walls Subjected to Cyclic Loading. *Journal of Earthquake Engineering, 15*(sup1), 30-71. doi:10.1080/13632469.2011.562049

Maffei, J., Bonelli, P., Kelly, D., Lehman, D. E., Lowes, L., Moehle, J., . . . Willford, M. (2014). *Recommendations for seismic design of reinforced concrete wall buildings based on studies of the 2010 Maule, Chile earthquake*. Retrieved from

Mejia, L., Ortiz, J., & Osorio, G. L. (2004). *Housing report—concrete shear wall buildings, report #109*. Retrieved from Colombia:

Paulay, T., & Priestley, M. J. N. (1992). *Seismic design of reinforced concrete and masonry buildings / T. Paulay, M.J.N. Priestley*: New York : Wiley, c1992.

Rosso, A., Jiménez-Roa, L. A., Almeida, J. P. d., Zuniga, A. P. G., Blandón, C. A., Bonett, R. L., & Beyer, K. (2018). Cyclic tensile-compressive tests on thin concrete boundary elements with a single layer of reinforcement prone to out-of-plane instability. *Bulletin of Earthquake Engineering, 16*(2), 859-887.

Sritharan, S., Beyer, K., Henry, R. S., Chai, Y. H., Kowalsky, M., & Bull, D. (2014). Understanding Poor Seismic Performance of Concrete Walls and Design Implications. *Earthquake Spectra, 30*(1), 307-334. doi:10.1193/021713EQS036M

Standards Australia. (2018). AS 3600-2018: Concrete Structures.

Sullivan, T. J., Priestley, M. J. N., & Calvi, G. M. (2012). *A Model Code for the Displacement-based Seismic Design of Structures*. Pavia, Italy: IUSS Press.